Electrical properties and stability of Dy_2O_3-doped ZnO–Pr_6O_{11}-based varistors

Choon-Woo Nahm

Abstract The electrical properties and DC accelerated aging characteristics of ZnO–Pr_6O_{11}-based varistors were investigated with various Dy_2O_3 contents and sintering times. It was found that the Dy_2O_3 content and sintering time significantly affected electrical properties and their stability. The nonlinear exponent with increasing Dy_2O_3 content varied with ∨-shaped, reaching maximum of 58.6 at 1.0 mol% Dy_2O_3 for varistors sintered for 1 h and with ∧-shaped, reaching maximum of 46.3 at 0.5 mol% Dy_2O_3 for 2 h. The leakage current was in the range of 0.1–1.1 μA for varistors sintered for 1 h and 0.3–2.4 μA for 2 h. The increase of sintering time led to lowering of nonlinearity. The varistors with 0.5 mol% Dy_2O_3 sintered for 2 h exhibited the good stability, under DC stress of 0.95 $V_{1\ mA}$/150 °C/24 h.

Introduction

Various electronic devices and electric power systems can be subjected to voltage transients (called surges) induced by lightning, switching, and electrostatic discharge. They are vulnerable to damage by surges in excess of their voltage ratings. Therefore, they should be protected from various surges. One way to overcoming surges is to enhance insulating strength for devices and systems. Another way is to use the varistors. Zinc oxide (ZnO) varistors are smart two-terminal semiconductor-ceramic devices made by sintering ZnO powder with small amounts of minor additives, necessarily containing varistor-forming oxides such as Bi_2O_3, Pr_6O_{11}, V_2O_5, BaO, La_2O_3, and so on [1, 2]. They exhibit highly nonlinear voltage-current (V-I) characteristics: electrical impedance of a varistor decreases abruptly at increasing voltage, and at a certain point, they behave as a short circuit. They possess excellent surge-energy-absorption capabilities. As a result, they have been extensively used to protect various semiconductor devices, electronic equipments, and electric power systems from dangerous abnormal high voltage [1, 2]. The nonlinear properties of ZnO varistors are attributed to a double Schottky barrier (DSB) formed at active grain boundaries containing many trap states.

Most commercial ZnO varistors contain Bi_2O_3 as VFO and they exhibit excellent varistor properties and high performance. However, they have a few drawbacks due to the high volatility and reactivity of Bi_2O_3 melted at about 825 °C during a sintering above 1000 °C [3]. The former changes varistor characteristics with the variation of inter-composition ratio of additives, the latter destroys the multi-layer structure of chip varistors, and it generates an insulating spinel phase deteriorating surge-absorption capabilities. Furthermore, they need many additives to obtain the high nonlinearity and stability.

In the past few years, it has been studying ZnO varistors containing Pr_6O_{11} as VFO to overcome these problems [4–15]. In the former work, Nahm et al. reported that ZnO–Pr_6O_{11}–CoO–Cr_2O_3–M_2O_3 (M = Er, Y)-based varistors exhibit high nonlinear properties and stability [8–14]. Many researchers who are

C.-W. Nahm (✉)
Department of Electrical Engineering, Dongeui University, Busan 614-714, Korea
e-mail: cwnahm@deu.ac.kr

interested in varistors wish to fabricate ZnO varistors exhibiting both higher nonlinearity and higher stability. But it is never easy. Therefore, it is very important to scrutinize the role of individual additive to apply ZnO–Pr_6O_{11}-based varistors in various areas.

The purpose of this work is to investigate the effect of Dy_2O_3 addition and sintering time on electrical properties and stability against DC accelerated aging stress of ZnO–Pr_6O_{11}–CoO–Cr_2O_3–Dy_2O_3-based varistors.

Experimental procedure

Sample preparation

Reagent-grade raw materials were used in proportions of (97.0-x) mol% ZnO, 0.5 mol% Pr_6O_{11}, 2.0 mol% CoO, 0.5 mol% Cr_2O_3, x mol% Dy_2O_3 (x = 0.5, 1.0, 2.0). Raw materials were mixed by ball milling with zirconia balls and acetone in a polypropylene bottle for 24 h. The mixture was dried at 120 °C for 12 h and calcined in air at 750 °C for 2 h. The calcined mixture was pulverized using an agate mortar/pestle and after 2 wt% polyvinyl alcohol (PVA) binder addition, granulated by sieving 200-mesh screen to produce starting powder. The powder was uniaxially pressed into discs of 10 mm in diameter and 2 mm in thickness at a pressure of 800 kg/cm^2. The discs were covered with raw powder in alumina crucible, sintered at 1350 °C in air for 1–2 h, and furnace-cooled to room temperature. The heating and cooling rates were 4 °C/min. The sintered samples were lapped and polished to 1.0 mm thickness. The size of the final samples was about 8 mm in diameter and 1.0 mm in thickness. Silver paste was coated on both faces of the samples and the ohmic contact of electrodes was formed by heating at 600 °C for 10 min. The electrodes were 5 mm in diameter.

Microstructure measurement

The either surface of samples was lapped and ground with SiC paper and polished with 0.3 μm-Al_2O_3 powder to a mirror-like surface. The polished samples were thermally etched at 1100 °C for 30 min. The surface of samples was metallized with a thin coating of Au to reduce charging effects and to improve the resolution of the image. The surface microstructure was examined by a scanning electron microscope (SEM, Hitachi S2400, Japan). The average grain size (d) was determined by the lineal intercept method by the following expression [16]:

$$d = 1.56L/MN \tag{1}$$

where L is the random line length on the micrograph, M is the magnification of the micrograph, and N is the number of the grain boundaries intercepted by lines. The density (ρ) of varistor ceramics was measured by the Archimedes method.

Electrical measurement

The voltage–current (V-I) characteristics of varistors were measured by stepping up the linear stair voltage in increment of 0.4–1.0 V using a high voltage source-measure unit (Keithley 237). To avoid joule heat of varistors, the varistors were applied up to 50 mA/cm^2. The varistor voltage ($V_{1\ mA}$) was measured at 1.0 mA/cm^2 and the leakage current (I_L) was measured at 0.80 $V_{1\ mA}$. In addition, the non-linear exponent (α) is calculated by the following equation:

$$\alpha = 1/(\log E_2 - \log E_1) \tag{2}$$

where E_1 and E_2 are the electric fields corresponding to 1.0 mA/cm^2 and 10 mA/cm^2, respectively.

The capacitance–voltage (C-V) characteristics of varistors were measured at 1 kHz with the variable applied bias in the pre-breakdown region of the V-I characteristics using a QuadTech 7600 RLC meter and a Keithley 617 electrometer. The donor concentration (N_d) of ZnO grains and the barrier height (ϕ_b) at the grain boundary were determined from the slope and intercept of straight line, respectively, using the following equation [17]:

$$(1/C_b - 1/2C_{bo})^2 = 2(\phi_b + V_{gb})/q\,\epsilon\,Nd \tag{3}$$

where C_b is the capacitance per unit area of a grain boundary, C_{bo} is the value of C_b when $V_{gb} = 0$, V_{gb} is the applied voltage per grain boundary, q is the electronic charge, ϵ is the permittivity of ZnO ($\epsilon = 8.5_{\epsilon o}$). The density of interface states (N_t) at the grain boundary was determined by the following equation [17]:

$$N_t = (2\,\epsilon\,N_d\phi_b/q)^{1/2} \tag{4}$$

Once the donor concentration and barrier height are known, the depletion layer width (t) of the either side at the grain boundaries was determined by the following equation [18]:

$$N_d t = N_t \tag{5}$$

DC accelerated aging test

The DC accelerated aging stress test was performed under four continuous conditions, such as 0.85 $V_{1\ mA}$/115 °C /24 h in 1st stress, 0.90 $V_{1\ mA}$/120 °C /24 h in 2nd stress, 0.95 $V_{1\ mA}$/125 °C /24 h in 3rd stress, and 0.95 $V_{1\ mA}$/150 °C /24 h in 4th stress. Simultaneously, the leakage current was monitored at intervals of 1 min during stressing using a high voltage source-measure unit (Keithley 237). The degradation rate coefficient (K_T) was calculated from the following equation [19]:

$$I_L = I_{Lo} + K_T t^{1/2} \tag{6}$$

where I_L is the leakage current at stress time (t) and I_{Lo} is I_L at $t = 0$. After the respective stresses, the V-I characteristics were measured at room temperature.

Results and discussion

Figure 1 shows SEM micrographs of ZPCCD-based ceramics with various Dy_2O_3 contents and sintering times. It is well known that the microstructure of Pr_6O_{11}-based ZnO varistor ceramics is consisted of only two phases [20]; as indicated in Fig. 1, ZnO grain (bulk phase, blackish) and intergranular layer (second phase, whitish). The SEM micrographs remarkably show two phases, ie. ZnO grains and intergranular layers regardless of Dy_2O_3 content and sintering time. Intergranular layers were Dy- and Pr-rich phases by XRD analysis. It was found from EDX that they coexist at the grain boundaries and the nodal points as if they were a single phase. It was observed by SEM that as the Dy_2O_3 content increased, the intergranular phase gradually more distributed at the grain boundaries and particularly the nodal points. These microstructures are not greatly

Fig. 1 SEM micrographs of ZPCCD-based ceramics with various Dy_2O_3 contents and sintering times
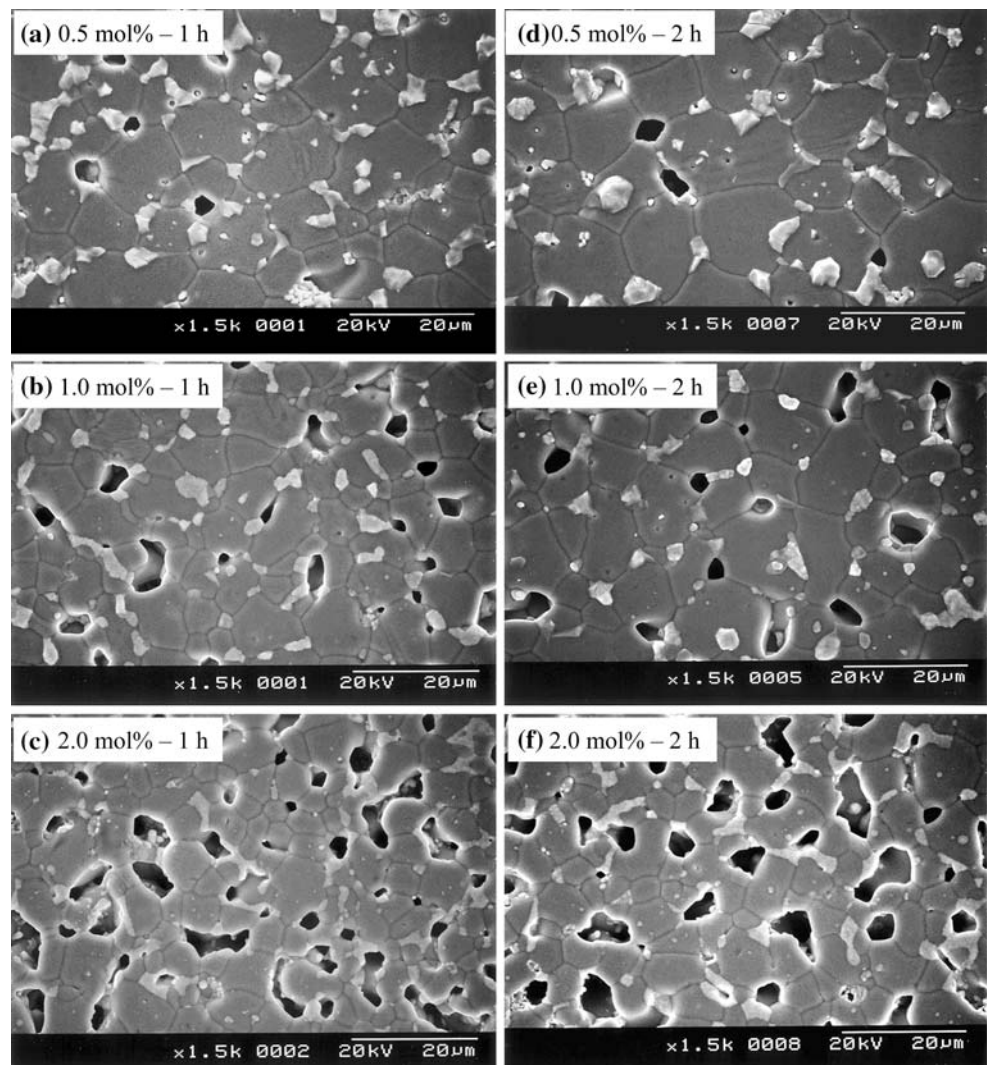
different from ZPCCM (M = Er, Y) reported previously [8, 11].

The detailed parameters are summarized in Table 1. With increasing Dy_2O_3 content, the average grain size of ceramics sintered for 1 h decreased in the range of 14.5–4.6 μm and 16.5–5.3 μm for 2 h. Therefore, the Dy_2O_3 was found to serve as an inhibitor of grain growth. It was found that the density of ceramics sintered for 1 h is in the range of 5.49–4.64 g/cm³ corresponding to 95.0–80.3% of theoretical density (TD = 5.78 g/cm³ in ZnO) and 5.58–4.72 g/cm³ corresponding to 96.5–81.7% of TD for 2 h. The density of ceramics decreased with increasing Dy_2O_3 for both sintering times. On the whole, the ceramics sintered for 2 h were slightly densified than those sintered for 1 h. The density greatly affects the resistance of degradation, together with a leakage current in the V-I characteristics. As we should discuss later, generally the lager the density, the higher the stability.

Figure 2 shows the electric field–current density (E-J) characteristic curves of varistors with various Dy_2O_3 contents and sintering times. For both sintering times, the current density increased linearly in low field, whereas it varied by orders of magnitude with only small changes in field above the breakdown field, called a varistor voltage. The variation of V-I characteristic parameters, including the varistor voltage ($V_{1\,mA}$), varistor voltage per grain boundary (V_{gb}), nonlinear exponent (α), and leakage current (I_L) are summarized in Table 1. As the Dy_2O_3 content increased, the $V_{1\,mA}$ and $V_{1\,mA}$ per grain boundary were found to increase in the range of 181.9–481.0 V/mm for varistors sintered for 1 h and 150.3–372.3 V/mm for 2 h. The $V_{1\,mA}$ is directly related to the number of grain boundaries across a series between the electrodes. Therefore, as the Dy_2O_3 content increased, the increase of $V_{1\,mA}$ is attributed to the decrease of average grain size caused by Dy_2O_3 addition inhibiting grain growth, as mentioned when discussing microstructure previously. By the same reasoning, it can be seen that the $V_{1\,mA}$ decreased by a longer sintering
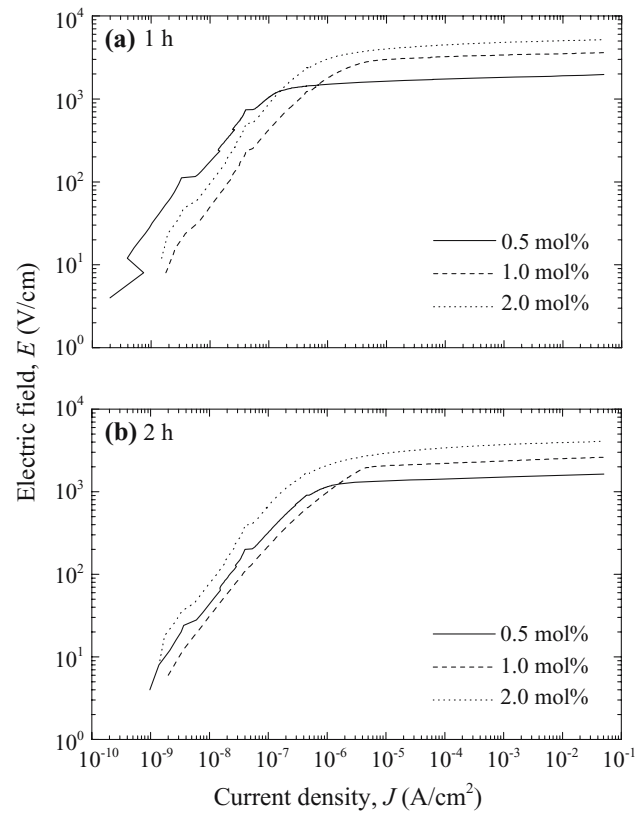
Fig. 2 E-J characteristics of ZPCCD-based varistors with various Dy_2O_3 contents and sintering time

time. The V_{gb} that is a breakdown voltage per grain boundaries is defined by the following equation:

$$V_{gb} = (d/D)_{1mA} \tag{7}$$

where d is the average grain size and D is the thickness of the sample. It was in the range of 2.2–2.9 V/gb for the varistors sintered for 1 h and 2.0–2.6 V/gb for 2 h with Dy_2O_3 content. This was within the generally well-known 2–3 V/gb regardless of sintering processes.

One of the most important figures of merit in varistors is the α, which characterizes the native properties of varistors itself. The α value varied with

Table 1 Microstructure, V-I, and C-V characteristic parameters of ZPCCD-based varistors with various Dy_2O_3 contents and sintering times

| Sintering time	Dy_2O_3 content (mol%)	d (μm)	ρ (g/cm³)	$V_{1\,mA}$ (V/mm)	V_{gb} (V/gb)	α	I_L (μA)	N_d (10^{18}/cm³)	N_t (10^{12}/cm²)	ϕ_b (eV)	t (nm)
1 h	0.5	14.5	5.49	181.9	2.6	55.3	0.1	1.06	3.15	1.00	29.8
	1.0	8.4	5.16	338.3	2.9	58.6	0.7	0.84	2.66	0.90	31.9
	2.0	4.6	4.64	481.0	2.2	48.8	1.1	0.25	1.39	0.82	55.4
2 h	0.5	16.5	5.58	150.3	2.5	46.3	0.3	1.52	3.59	0.91	23.7
	1.0	11.0	5.41	235.6	2.6	35.1	0.8	1.18	2.91	0.76	24.6
	2.0	5.3	4.72	372.0	2.0	39.4	2.4	0.57	1.81	0.61	31.6

∨-shaped in the range of 48.8–58.6 for the varistors sintered for 1 h. As the Dy_2O_3 content increased, the α value increased up to 1.0 mol%, reaching a maximum value (58.6) close to 60 at 1.0 mol%, whereas more contents decreased α value. On the other hand, the α value varied with ∧-shaped in the range of 35.1–46.3 for the varistors sintered for 2 h. As the Dy_2O_3 content increased, the α value decreased up to 1.0 mol%, reaching a minimum value (35.1) close to 35 at 1.0 mol%, whereas more contents decreased the α value. The maximum value of α was obtained from the varistors doped with 0.5 mol% Dy_2O_3, reaching $\alpha = 46.3$. The increase of sintering time in equivalent compositions will lead to the low nonlinearity. However, the stability may be improved due to the increase of density. The I_L values increased in the range of 0.1–1.1 μA in varistors sintered for 1 h and of 0.3–2.4 μA for 2 h, with a minimum value at 0.5 mol% Dy_2O_3 for both sintering times. The I_L value for the varistors sintered for 2 h exhibited to be high than that for 1 h. However, on the whole, the I_L value for these varistors is estimated to be low.

Figure 3 shows the C-V characteristics of varistors with various Dy_2O_3 contents and sintering times. It is assumed that the C-V characteristics for sintering time will be various because the C-V characteristic curves are arranged variously according to various Dy_2O_3
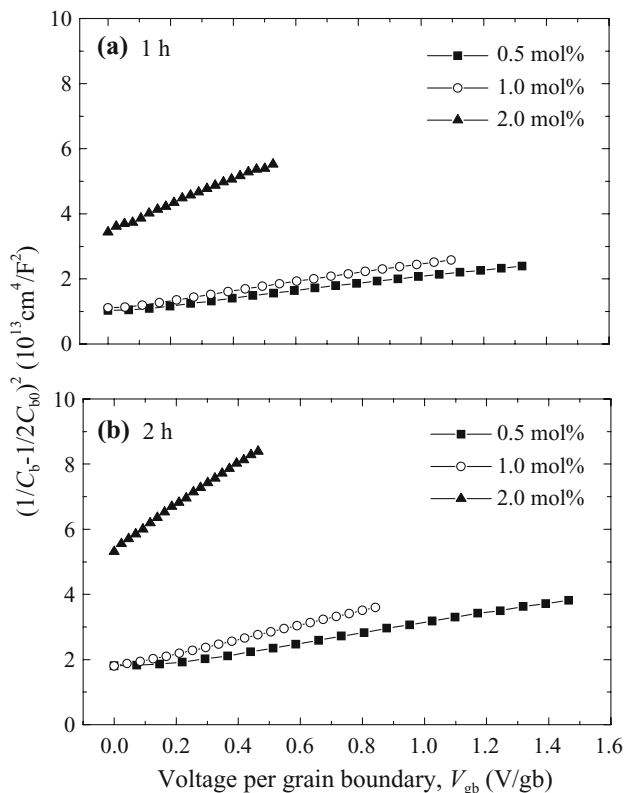
Fig. 3 C-V characteristics of ZPCCD-based varistors with various Dy_2O_3 contents and sintering times

contents and sintering times. The C-V characteristic parameters, including the donor concentration (N_d), density of interface states (N), barrier height (ϕ_b), and depletion layer width (t) are summarized in Table 1. As the Dy_2O_3 content increased, the N_d value decreased in the range of 1.06×10^{18}–0.25×10^{18} cm^{-3} for varistors sintered for 1 h and in the range of 1.52×10^{18}–0.57×10^{18} cm^{-3} for 2 h. These do not greatly differ from general $\sim 10^{18}$ orders of magnitude. The decrease of N_d with increasing Dy_2O_3 content exhibited the same tendency as the ZnO–Pr_6O_{11}–CoO–R_2O_3 (R = Dy, Er) system with no Cr_2O_3 [4, 5]. Although Dy^{+3} ions have a larger radius (0.091 nm) than Zn^{+2} ions (0.074 nm), thus limited substitution within the ZnO grains is possible. Dy substitutes for Zn and creates lattice defects in ZnO grains. The chemical-defect reaction using Kroger–Vink notation can be written as follow equation:

$$Dy_2O_3 \xrightarrow{ZnO} 2Dy_{Zn}^{\bullet} + V_{Zn}'' + 3O_O^{\times} \tag{8}$$
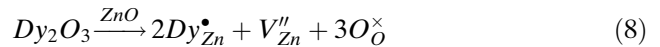
where $Dy_{Zn}^{\bullet}$ is a positively charged Dy ion substituted for a Zn lattice site, V_{Zn}'' is a negatively charged Zn vacancy, and $O_O^{\times}$ is a neutral oxygen of an oxygen lattice site. A negatively charged zinc vacancy (V_{Zn}''), could act as a donor, gaining hole to become either singly positively charged or a neutral zinc vacancy. This would cause net donor concentration to increase. However, the donor concentration decreased according to experimental results. Presumably, it is assumed that the addition of Dy_2O_3 leads to the decrease of zinc interstitial or oxygen vacancy concentration acting as natural donors due to any reason. The reason needs to further deeply investigated.

The N_t value decreased in the range of 3.15×10^{12}–1.39×10^{12} cm^{-2} for the varistors sintered for 1 h and 3.59×10^{12}–1.81×10^{12} cm^{-2} for 2 h with increasing Dy_2O_3 content. The ϕ_b value decreased in the range of 1.0–0.82 eV for the varistors sintered for 1 h and in the range of 0.91–0.61 eV for 2 h with increasing Dy_2O_3 content. On the whole, the ϕ_b value of varistors sintered for 2 h exhibited to be lowered compared with those for 1 h. It is assumed that the lowering of ϕ_b value gives rise to low nonlinearity, when comparing with the nonlinear exponent (α) between varistors sintered for 1 h and 2 h.

ZnO varistors begin to degrade because of gradually increasing leakage current with stress time. Eventually, they result in thermal runaway from stems joule heating and the loss of varistor function. From this viewpoint, in addition to nonlinearity, the electrical stability is a technologically very important characteristic of ZnO varistors.

Figure 4 shows the variation of leakage current of varistors during various DC accelerated aging stresses

with various Dy_2O_3 contents and sintering times. As shown in I_L-$t^{1/2}$ curves, the varistors doped with 1.0 and 2.0 mol% Dy_2O_3 sintered for 1 h exhibited thermal runaway within a short time under 1st stress. This unstable state is attributed to the low density, that is, the low density leads to the concentration of current through the limited conduction path and further high current density per grain boundary. This means that the density more predominantly affects the stability, compared with the leakage current. On the contrary, it can be seen that the varistor doped with 0.5 mol% Dy_2O_3 sintered for 1 h exhibit remarkably high stability without a thermal runaway. Their leakage current was nearly constant until third stress and shows very weak positive creep during fourth stress. On the other hand, the varistors sintered for 2 h exhibited high stability without thermal runaway up to 1.0 mol% Dy_2O_3. But the varistors doped with 0.5 mol% Dy_2O_3 revealed higher leakage current than that sintered for 1 h. There is need to compare the stability for only varistors doped with 0.5 mol% Dy_2O_3. The stability of varistors against DC accelerated aging stress can be estimated from the degradation rate coefficient (K_T).

The K_T value increased as DC accelerated aging stress became more severe, and increased abruptly after 4th stress. After 4th stress, the K_T value was 2.31 $\mu A \cdot h^{-1/2}$ in the varistor sintered for 1 h and 1.33 $\mu A \cdot h^{-1/2}$ in the varistor sintered for 2 h. This suggests the varistor sintered for 2 h will exhibit higher stability comparatively, compared with that for 1 h. Furthermore, the detailed variation rate of V-I characteristic parameters after various DC accelerated aging stresses is summarized in Table 2. The varistor with 0.5 mol% Dy_2O_3 sintered for 1 h revealed the %$\Delta V_{1\,mA}$ (variation rate of $V_{1\,mA}$) of –0.8%, the %$\Delta\alpha$ (variation rate of α) of –14.3%, and the %ΔI_L (variation rate of I_L) of +600% after 4th stress. It can be seen that The $V_{1\,mA}$ was very stable state, whereas the α and I_L were comparatively unstable state for stress. On the contrary, the varistor with 0.5 mol% Dy_2O_3 sintered for 2 h revealed the %$\Delta V_{1\,mA}$ of –2.9%, the %$\Delta\alpha$ of –4.1%, and the %ΔI_L of + 166.7% after fourth stress. The stability of the nonlinear exponent and leakage current was found to be well above three times than that sintered for 1 h. In general, the stability against DC accelerated aging stress is high, as the ceramics are

Fig. 4 Leakage current of ZPCCD-based varistors during various DC accelerated aging stresses with various Dy_2O_3 contents and sintering times.
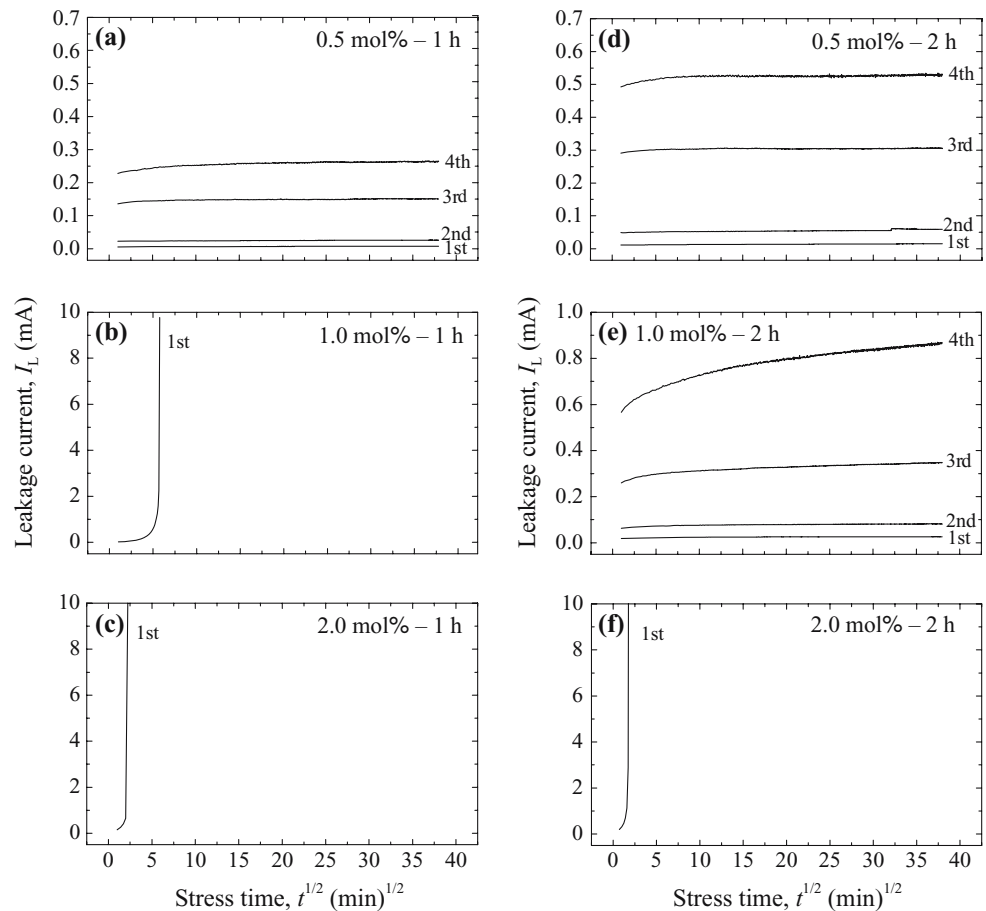
Table 2 Variation of *V-I* characteristic parameters after various DC accelerated aging stresses of ZPCCD-based varistors with various Dy$_2$O$_3$ contents and sintering times

Sintering time	Dy$_2$O$_3$ content (mol%)	Stress state	$V_{1\,mA}$ (V/mm)	%$\Delta V_{1\,mA}$	α	%$\Delta\alpha$	I_L (μA)	%ΔI_L
1 h	0.5	Before	181.9	0	55.3	0	0.1	0
		1st	180.1	–1.0	53.4	–3.4	0.3	200.0
		2nd	179.6	–1.3	52.9	–4.3	0.3	200.0
		3rd	179.0	–1.6	51.8	–6.3	0.4	300.0
		4th	180.4	–0.8	47.4	–14.3	0.7	600.0
	1.0	Before	338.3	0	58.6	0	0.7	0
		1st	Thermal runaway					
	2.0	Before	481.0	0	48.8	0	1.1	0
		1st	Thermal runaway					
2 h	0.5	Before	150.3	0	46.3	0	0.3	0
		1st	148.1	–1.5	43.6	–5.8	0.4	33.3
		2nd	147.0	–2.2	43.3	–6.5	0.5	66.7
		3rd	146.4	–2.6	43.0	–7.1	0.5	66.7
		4th	145.8	-2.9	44.4	-4.1	0.8	166.7
	1.0	Before	235.6	0	35.1	0	0.8	0
		1st	232.7	-1.2	33.7	-4.0	1.1	37.5
		2nd	230.8	-2.0	31.6	-10.0	1.4	75.0
		3rd	228.8	-2.9	29.7	-15.4	1.9	137.5
		4th	230.2	-2.3	25.9	-26.2	2.7	237.5
	2.0	Before	372.0	0	39.4	0	2.4	0
		1st	Thermal runaway					

densified and the leakage current is lowered. The varistor sintered for 2 h with 0.5 mol% Dy$_2$O$_3$ have high density and high leakage current, compared with that for 1 h. Consequently, it can be seen that the combination of proper Dy$_2$O$_3$ content and sintering time leads to high nonlinearity and stability.

The defect model proposed by Gupta and Carlson can be usefully used in discussing stability of varistors [21]. The key of degradation under external stress results from deformation of Schottky barrier between ZnO grains. The factors relating to degradation are meta-stable ions such as zinc interstitial ion in depletion region. These ions are relatively mobile compared with other ions. The Zn$_i$ is diffused toward grain boundaries under external stress and reacts with negatively charged Zn vacancy. As a result, this process leads to a reduction of potential barrier and an increase of leakage current. Therefore, the way to improve the stability is to restrict the generation of Zn$_i$ within depletion layer or the migration of Zn$_i$ toward grain boundaries. Presumably, it is assumed that the proper Dy$_2$O$_3$ incorporation and sintering time are related to the migration of zinc interstitial (Zn$_i$) within depletion layer or the stabilization of interface states.

Conclusions

The electrical properties and the stability of nonlinear properties against DC accelerated aging stress of varistors, which are composed of ZnO–Pr$_6$O$_{11}$–CoO–Cr$_2$O$_3$–Dy$_2$O$_3$ systems, were investigated with various Dy$_2$O$_3$ contents and sintering times. The density of ceramics increased with increasing sintering time, whereas it decreased with increasing Dy$_2$O$_3$ content. As the Dy$_2$O$_3$ content increased, the nonlinear exponent changed with ∨-shaped in the range of 48.8–58.6, reaching maximum (58.6) at 1.0 mol% Dy$_2$O$_3$ for varistors sintered for 1 h and with ∧-shaped in the range of 35.1–46.3, reaching maximum (58.6) at 0.5 mol% Dy$_2$O$_3$ for varistors sintered for 2 h. The leakage current increased in the range of 0.1–1.1 μA for varistors sintered for 1 h and of 0.3–2.4 μA for 2 h. A longer sintering time decreased the nonlinear properties, whereas it improved the stability against DC accelerated aging stress in the equivalent Dy$_2$O$_3$ content. In particular, the varistor doped with 0.5 mol% Dy$_2$O$_3$ sintered for 2 h exhibited a good stability, in which %$\Delta V_{1\,mA}$ = –2.9%, %$\Delta\alpha$ = –4.1%, and %ΔI_L = + 166.7% under DC accelerated aging stress such as 0.95 $V_{1\,mA}$/150 °C /12 h.

References

1. Levinson LM, Pilipp HR (1986) Am Ceram Soc Bull 65:639
2. Gupta TK (1990) J Am Ceram Soc 73:1817
3. Lee YS, Tseng TY (1992) J Am Ceram Soc 75:1636
4. Nahm CW (2001) J Euro Ceram Soc 21:545
5. Nahm C-W, Park C-H (2001) J Mater Sci 36:1671
6. Nahm C-W, Yoon H-S, Ryu J-S (2001) J Mater Sci Lett 20:393
7. Nahm C-W (2001) Mater Lett 47:182
8. Nahm C-W, Ryu J-S (2002) Mater Lett 53:110

9. Nahm C-W, Shin B-C (2002) J Mater Sci : Mater Electro 12:111
10. Nahm C-W (2003) Mater Lett 57:1317
11. Nahm C-W, Shin B-C (2003) Mater Lett 57:1322
12. Nahm NC-W, Kim H-S (2003) Mater Lett 57:1544
13. Nahm C-W (2003) J Euro Ceram Soc 23:1345
14. Nahm C-W, Shin B-C, Min B-H (2003) Mater Chem and Phys 82:157
15. Nahm C-W (2003) Solid State Commun1 27:389
16. Wurst JC, Nelson JA (1972) J Am Ceram Soc 97–12:109
17. Mukae M, Tsuda K, Nagasawa I (1979) J Appl Phys 50:4475
18. Hozer L (1994) In Semiconductor ceramics: grain boundary effects. Ellis Horwood, pp 22
19. Fan J, Freer R (1995) J Appl Phys 77:4795
20. Mukae K (1987) Am Ceram Soc Bull 66:1329
21. Gupta TK, Carlson WG (1985) J Mat Sci 20:3487